ORIGINAL PAPER
Polish Journal of Microbiology
2025, Vol. 74, No 3, 374-384
https://doi.org/10.33073/pjm-2025-032

Identification of a Novel Haloarchaeal Species *Halorubellus amylolyticus* sp. nov., Isolated from Salt Crystals of Salted Seaweed Knots and Genomic Insights into Genus *Halorubellus*

YAWEN LIU[1#], AODI ZHANG[1,2#], JINQIANG MA[1], CUNLONG LU[1], SHILONG SHAO[1], YUE DING[1], YULING HAO[1], YU JIN[1], JINGFANG LIU[3], LIANG SHEN[1] and SHAOXING CHEN[1*]

[1]College of Life Sciences, Anhui Normal University, Wuhu, P. R. China
[2]Xiaoxian Experimental Senior High School, Xiaoxian, P. R. China
[3]Institutional Center for Shared Technologies and Facilities of Institute of Microbiology, Chinese Academy of Sciences, Beijing, P. R. China

Submitted 26 July 2025, accepted 8 August 2025, published online 18 September 2025

Abstract

An extremely halophilic archaeon named strain PRR65^T was isolated from a salt crystal of salted seaweed knots which were purchased from a supermarket in Wuhu, China. It exhibited an ability to hydrolyze starch. Strain PRR65^T is a coccus. Its growth range and optimum concentration for NaCl are 2.0–5.1 M and 3.4 M, respectively, and it requires magnesium ions (with an optimum concentration of 0.01 M). Homology search of the 16S rRNA gene sequence indicated that strain PRR65^T shows the highest sequence similarities with *Halorubellus salinus* GX3^T (96.97%). The basic growth conditions and many other physicochemical characteristics of strain PRR65^T are distinct from those of other species within its genus. The average nucleotide identity (ANI), average amino acid identity (AAI), and digital DNA-DNA hybridization (dDDH) values between strain PRR65^T and its close relatives were 88.97%, 86.47% and 39.2%, respectively. The DNA G + C content (mol%) for strain PRR65^T is 67.2%. Based on a polyphasic taxonomic approach integrating phenotypic characteristics, chemotaxonomic markers, and comprehensive phylogenetic and genomic analyses, strain PRR65^T represents a novel species within the genus *Halorubellus*. The name *Halorubellus amylolyticus* sp. nov. is proposed, with the specific epithet reflecting the organism's notable amylolytic activity. The type strain is PRR65^T (= MCCC 4K00175 = KCTC 4323).

Keywords: Haloarchaea, *Halorubellus*, hypersaline environments, polyphasic taxonomy, salt crystal

Introduction

Natural hypersaline environments are widely distributed on Earth, including salt lakes, saline-alkali soils, solar salterns, inland saltworks, salt mines, and others (Ding et al. 2025). Halophilic archaea predominantly inhabit these hypersaline environments (Ventosa et al. 2015; Baker et al. 2024). Due to the widespread use of crude salts from solar salterns in food fermentation processes, large numbers of halophilic archaea have also been discovered in many salted foods. Strain PRR65, a member of the genus *Halorubellus*, is one such halophilic archaeon isolated from salt crystals of salted seaweed knots and exhibits extracellular protease activity. The extracellular protease encoding gene of strain PRR65, *hly65*, was identified, and the kinetic parameters of Hly65 have been characterized (Hao et al. 2024). The genus *Halorubellus*, belonging to the family *Halobacteriaceae*, was established by Cui et al. (2012). Thirteen years have passed, and this ge-

# Yawen Liu and Aodi Zhang contributed equally to this study.
* Corresponding author: Shaoxing Chen, College of Life Sciences, Anhui Normal University, Wuhu, P. R. China; **email: chensx@ahnu.edu.cn**

nus still comprises only two recognized species with validly published names, namely *Halorubellus salinus* and *Halorubellus litoreus* (Cui et al. 2012). Recently, through 16S rRNA gene and *rpoB'* gene sequence similarity analyses combined with phenotypic characterization, we have tentatively proposed that strain PRR65^T likely represents a novel species within this genus. In this study, we will conduct the polyphasic taxonomic characterization of strain PRR65^T according to the newly updated proposal described by Cui et al. (Cui et al. 2024).

Experimental

Materials and Methods

Culture medium and cultivation conditions. The strain PRR65^T was isolated from salted seaweed salt crystals purchased from a supermarket in Wuhu City, China (118.3797326°E, 31.3422958°N). The isolation procedure was performed using a neutral oligotrophic halophilic archaeal medium (NOM) with the following composition (g/l): $MgSO_4 \cdot 7H_2O$ 20, KCl 2.0, trisodium citrate 3.0, sodium glutamate 1.8, NaCl 150, $FeSO_4 \cdot 7H_2O$ 0.05, $MnCl_2 \cdot 4H_2O$ 0.036, Bacto™ Casamino Acids 1.0, yeast extract 1.0, and sodium pyruvate 1.0 (pH 7.2) (Cui et al. 2010). Solid medium was prepared by adding 2% agar to the liquid medium, and isolation was conducted via streak plating on NOM agar plates. Unless otherwise specified, strain PRR65^T was cultivated at 38°C (with shaking at 180 rpm for liquid cultures).

Phenotypic analysis. Comprehensive characterization of colonial morphotypes was conducted using direct plate observation under calibrated optical microscopy. An phase-contract optics (Leica DMI6000 B) was employed to check cell morphology under optimal growth conditions (3.4 M NaCl, 38°C) after cultivation on the NOM. Gram staining was conducted following the protocol described by Dussault (1955). Bacterial motility was assessed using the stab inoculation method in semi-solid NOM medium columns.

The phenotypic characterization of strain PRR65^T was conducted in accordance with the proposed minimal standards for describing new taxa of the class *Halobacteria* (Cui et al. 2024). The cellular morphology of the four strains was observed using phase-contrast microscopy and scanning electron microscopy, with Gram staining performed using a modified technique (Dussault 1955). The salinity range for growth was determined using modified NOM medium with a NaCl concentration gradient of 0.85–5.1 M (increments of 0.34 M). The temperature gradient was set at 15, 20, 25, 30, 35, 38, 40, 45, 50, and 55 °C. pH adaptability was assessed within a range of pH 5.0–9.5 at 0.5 intervals using different biological buffer systems (Chen et al. 2015). The magnesium dependence profile of strain PRR65^T was quantitatively determined using a modified neutral oligotrophic medium (NOM) formulation. To establish precise tolerance limits, the standard $MgSO_4$ component was systematically replaced with $MgCl_2$ at final concentrations spanning four orders of magnitude: 0, 0.005, 0.01, 0.05, 0.1, 0.2, 0.3, 0.4, 0.5, 0.6, 0.7, 0.8, and 1.0 M. Triplicate cultures were incubated under optimal growth conditions (3.4 M NaCl, pH 7.0, 38°C) with growth kinetics monitored spectrophotometrically at OD_{600} over 14 days. Minimum salt requirements for cellular integrity were established through hypotonic challenge assays. Exponentially growing cells were harvested, washed three times in basal buffer (20 mM Tris-HCl, pH 7.2), and resuspended in NaCl gradients (0–2.0 M in 0.25 M increments). Membrane stability was evaluated through two complementary methods: i) quantitative measurement of cell lysis via OD_{600} decay over 120 minutes, and ii) qualitative viability assessment through spot-plating 10-µl aliquots onto NOM agar followed by 7-day incubation. The critical osmotic threshold was defined as the lowest NaCl concentration maintaining > 90% OD_{600} stability and colony-forming capability. The following characteristics were examined according to the methods of Cui et al. (2012): nitrate-dependent growth with gas production, nitrate reduction with gas production, anaerobic growth with KNO_3/L-arginine/DMSO (5 g/l), starch hydrolysis, gelatin hydrolysis, esterase activity, catalase and oxidase activity, and H_2S production from cysteine. Indole production, utilization of single carbon sources, and antibiotic susceptibility were determined following the methods of Chen et al. (2015). Acid production from single carbon sources was tested using an unbuffered NOM liquid medium. Polar lipids were extracted using a chloroform/methanol system and analyzed by one- and two-dimensional thin-layer chromatography (TLC) (Chen et al. 2015).

Sequence similarity analysis. The *rpoB'* gene of strain PRR65^T was amplified and sequenced with the same primer pair HrpoB2 1420F (5′ TGTGGGCTNGTGAAGAACTT3′) and HrpoA 153R (5′GGGTCCATCAGCCCCATGTC3′) using a single colony as

PCR template (Minegishi et al. 2010). Sequence similarity was determined using the option of "Align two or more sequences" on the blastn suite (https://blast.ncbi.nlm.nih.gov/Blast.cgi).

Phylogenetic analysis. For comprehensive phylogenetic reconstruction, 16S rRNA and *rpoB'* gene sequences of all validly described *Halorubellus* species and phylogenetically neighboring taxa were systematically curated. Reference sequences were sourced from two complementary approaches: i) direct retrieval from the NCBI GenBank database (https://www.ncbi.nlm.nih.gov/genbank), and ii) extensive BLASTn searches (v2.13.0+) against the nt/nr databases using strain PRR65^T sequences as queries (E-value threshold < 1×10^{-50}). This dual-strategy ensured maximal coverage of taxonomically relevant sequences for subsequent comparative analysis. Multiple sequence alignments were performed using the CLUSTAL W program (Aiyar 2000) integrated into the BioEdit software (Hall 1999). Phylogenetic analyses based on a single gene, for instance the 16S rRNA gene or *rpoB'* gene, were conducted using MEGA 7 software (Kumar et al. 2016). Phylogenetic trees were reconstructed using three algorithms: maximum-likelihood (ML), neighbour-joining (NJ), and maximum-parsimony (MP). Bootstrap analysis with 1,000 replicates was performed in MEGA 7 to assess the robustness of the tree topologies.

Genome sequencing. Total genomic DNA was extracted following the method described by Cline et al. (1989), and genome sequencing was performed on the Illumina® HiSeq 4000 platform. The quality of sequencing reads was assessed using FastQC software (Brown et al. 2017), and the filtered high-quality reads were assembled into contigs using SPAdes software (Prjibelski et al. 2020). Genome completeness and contamination were evaluated using the CheckM tool (Parks et al. 2015).

Genome assembly, annotation, and comparative genomics analysis. Genome annotation was conducted with PROKKA software (Seemann 2014). COG categories were assigned with the online version eggNOG-mapper with default options (http://eggnog-mapper.embl.de). The pan-genome was constructed using PEPPAN v1.0.5 with default options and the gff files produced by PROKKA as the input. The result produced by the main program of PEPPAN was parsed using PEPPAN_parser with the arguments -t -c -a 95 and leaving others as their defaults (Zhou et al. 2020). ANI analysis was performed using the ANI Calculator web tool (https://www.ezbiocloud.net/tools/ani), while AAI was calculated using CompareM software (https://github.com/dparks1134/CompareM). The dDDH values were determined using the Genome-to-Genome Distance Calculator (GGDC) 4.0 platform (https://ggdc-test.dsmz.de/ggdc.php).

Phylogenomic analysis. The phylogenomic tree was reconstructed using EasyCGTree software (Zhang et al. 2023).

Results and Discussion

Phenotypic characteristics. Key differential features between strain PRR65^T and phylogenetically related *Halorubellus* species are comprehensively summarized in Table I. Colonial morphology analysis revealed moist, pale red colonies with smooth margins and slight convexity (elevation approximately 0.2–0.3 mm), reaching diameters of 0.5–1.0 mm after standard incubation (Fig. S1). Ultrastructural examination via phase-contrast optics confirmed uniformly spherical cell morphology for strain PRR65^T (Fig. 1), contrasting with the pleomorphic cellular structure characteristic of its closest relatives. The strain demonstrated a halo-adaptation profile distinct from related taxa, requiring NaCl concentrations between 2.0–5.1 M for growth, notably exhibiting a higher minimum salt requirement (2.0 M) compared to reference strains. Differential carbon metabolism was observed: acid production occurred during utilization of D-mannose, D-galactose, or D-fructose as sole carbon sources, whereas metabolism of D-glucose, sucrose, and starch proceeded without medium acidification. Antimicrobial susceptibility testing demonstrated that PRR65^T was sensitive to bacitracin (0.04 IU), novobiocin (5 μg), rifampicin (5 μg), and vancomycin (30 μg), but resistant to ampicillin (10 μg), chloramphenicol (30 μg), ciprofloxacin (5 μg), erythromycin (15 μg), norfloxacin (10 μg), penicillin G (10 IU), streptomycin (10 μg), kanamycin (30 μg), tetracycline (30 μg), and neomycin (30 μg). Polar lipid analysis by two-dimensional TLC confirmed a profile comprising phosphatidic acid (PA), phosphatidylglycerol (PG), phosphatidylglycerol phosphate methyl ester (PGP-Me), sulfated mannosyl glucosyl diether (S-DGD-1), mannosyl glucosyl diether (DGD-1), and sulfated galactosyl mannosyl glucosyl diether (S-TGD-1) as major components (Fig. S2). This lipid signature aligns with genus-level characteristics while exhibiting quantitative differences from related species.

Table I
Differential characteristics of strain PRR65^T and its closely related species within the genus *Halorubellus*.

Characteristics	1	2	3
Shape	Cocci	Pleomorphic	Polymorphic
NaCl range (M)	2.0–5.1	1.4–5.1	1.4–5.1
Optimum NaCl (M)	3.4	3.1	3.1
Mg^{2+} requirement	+	–	–
Optimum Mg^{2+}(M)	0.01	0.05	0.05
Anaerobic growth in:			
L-arginine	+	–	–
KNO_3	+	–	–
Utilization of			
D-glucose	+	–	–
D-mannose	+	–	–
D-galactose	+	–	+
Starch	+	–	+
Mannitol	+	–	–
Sorbitol	+	–	–
Lactate	–	–	+
Succinate	–	+	–
Malate	–	–	+
Citrate	–	–	+
L-alanine	+	–	+
L-lysine	–	+	–
Gelatin hydrolysis	–	+	+
H_2S formation	–	+	+
Oxidase activity	–	+	+
G + C content (mol%)	67.2	67.3	67.2

Taxa: 1 – Strain PRR65T; 2 – *Halorubellus salinus* GX3T; 3 – *Halorubellus litoreus* GX26T
Symbols: + positive; – negative

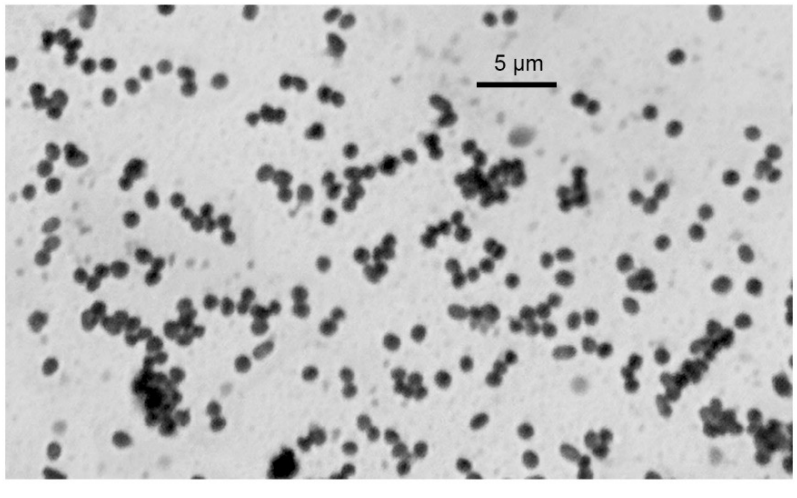

Fig. 1. Cell morphology of strain PRR65^T uncovered by a phase contrast optics (Leica DMI6000 B).

Supplementary physiological and biochemical characteristics that further delineate this taxon are provided in the formal species description. Collective phenotypic, genotypic, and chemotaxonomic evidence robustly supports the classification of PRR65^T as a novel species within the genus *Halorubellus*.

The 16S rRNA gene and *rpoB'* gene sequence similarity. A rigorous comparative analysis of the 16S rRNA gene sequence was conducted using the EzBioCloud database and NCBI BLAST (https://blast.ncbi.nlm.nih.gov/Blast.cgi). This examination revealed that strain PRR65^T shares its closest phylogenetic affinity with validly published species of the genus *Halorubellus*. Specifically, it demonstrated 96.97% 16S rRNA gene sequence similarity with the type strain *H. salinus* GX3^T and 96.36% similarity with *H. litoreus* GX26^T. These values fall below the conventional genus-level threshold (98.65%), suggesting potential novel species status. To further resolve taxonomic positioning, the evolutionarily conserved single-copy *rpoB'* gene was analyzed. Consistent with 16S rRNA phylogeny, strain PRR65^T exhibited 94.97% sequence similarity to *H. salinus* GX3^T and 95.30% similarity to *H. litoreus* GX26^T. This multi-locus approach robustly supports the classification of strain PRR65^T within the *Halorubellus* genus while distinguishing it from currently recognized species. Notably, while the 16S rRNA gene sequence similarity exceeded the species delineation threshold (98.65%) (Kim et al. 2014), and the *rpoB'* gene similarity met the required criteria.

Genome-based sequence relatedness. The basic information of the genomes of strains PRR65^T, *H. salinus* GX3^T, and *H. litoreus* GX26^T is listed in Table SI. The whole-genome ANI analysis yielded ANI values of 87.12% and 88.97% between strains PRR65^T and GX3^T/GX26^T, respectively. Corresponding average amino acid identity (AAI) values were 86.32% and 86.47% (Table II). These ANI values are significantly below the 95% species delineation threshold (Richter and Rosselló-Móra 2009), strongly supporting its classification as a novel species. dDDH analysis further confirmed this conclusion, with dDDH values of 32.7% and 39.2% between PRR65^T and GX3^T/GX26^T, respectively (Table II). According to DNA-DNA relatedness calculations, all dDDH values between PRR65^T and its closest relatives were below 40%, substantially lower than the 70% species delineation cutoff (Goris et al. 2007). Collectively, these genomic-level evidence conclusively demonstrates that PRR65^T represents a novel species within the genus *Halorubellus*.

Table II
Genome-based sequence similarity analysis between strain PRR65 and closely related species.

dDDH (%)\ANI (%)	1	2	3	4	5	6	7
1. PRR65		87.12	88.97	74.12	75.54	76.65	75.15
2. GX3	32.7		89.52	74.03	75.55	75.24	75.17
3. GX26	39.2	38.4		73.99	75.28	75.22	75.19
4. H22	19.9	19.9	20		75.15	75.04	75.11
5. YC82	16.2	20.9	21	20.4		88.12	78.72
6. KCTC 4080	21.4	20.7	20.9	20.2	34.4		78.50
7. XD48	20.7	20.5	20.7	20.3	22.2	21.9	

1 – *Halorubellus* sp. PRR65; 2 – *Halorubellus salinus* GX3; 3 – *Halorubellus litoreus* GX26; 4 – *Halomicrococcus hydrotolerans* H22; 5 – *Haloarchaeobius salinus* YC82; 6 – *Haloarchaebius iranensis* KCTC 4080; 7 – *Haloarchaebius amylolyticus* XD48; ANI – Average Nucleotide Identity; dDDH – digital DNA-DNA hybridization

Phylogenetic and phylogenomics analysis. Phylogenetic analysis based on 16S rRNA gene sequences demonstrated that strain PRR65^T exhibits the closest relationship with *H. salinus*, with a high bootstrap support value approaching 100% (Fig. 2a). In the 16S rRNA gene-based phylogenetic tree, PRR65^T initially clustered with *H. salinus* GX3^T to form a distinct branch, which subsequently grouped with *H. litoreus* GX26^T to constitute an independent evolutionary clade representing the genus *Halorubellus*. However, the *rpoB'*

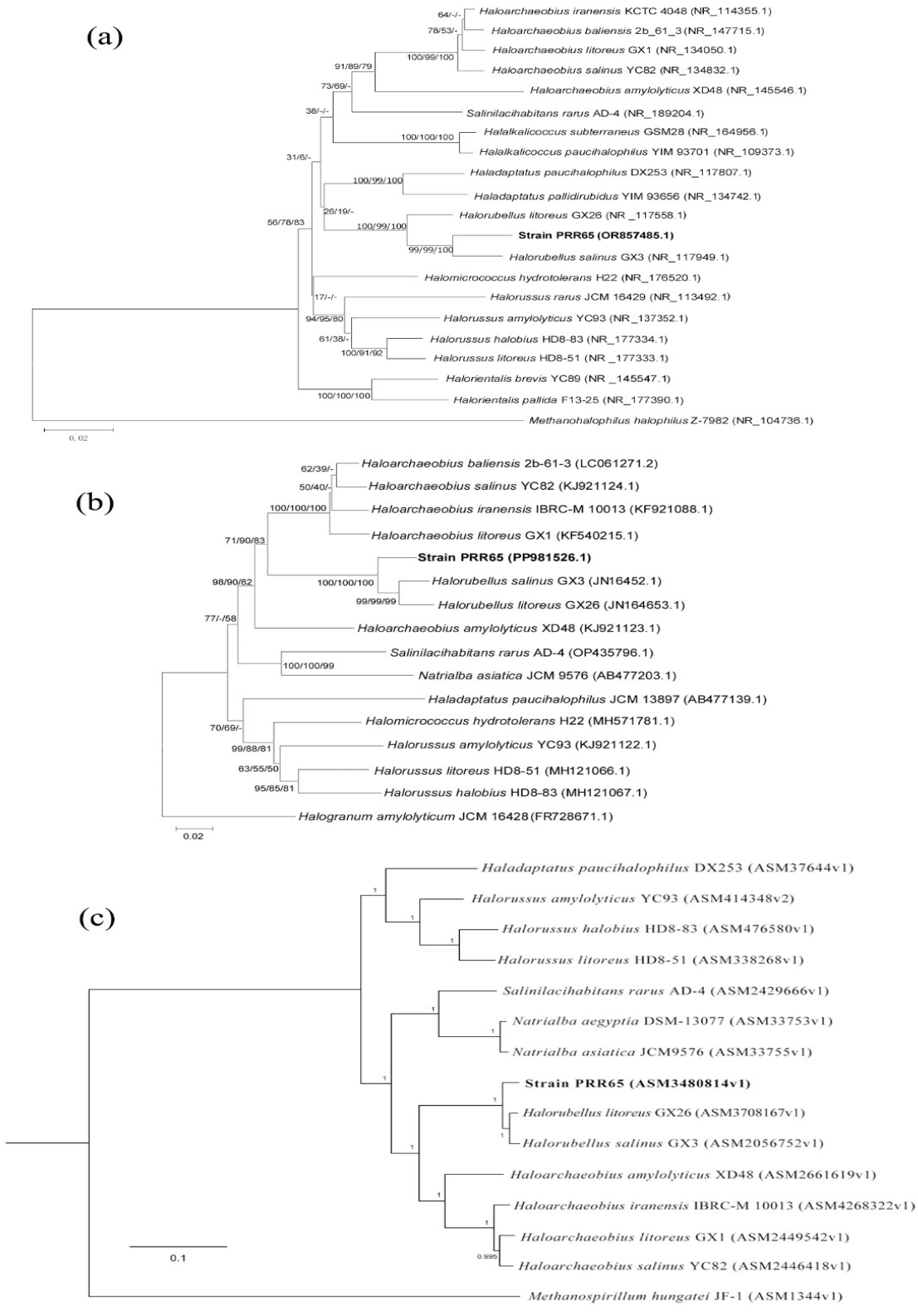

Fig. 2. Phylogenetic relationship reconstruction based on the 16S rRNA gene (a) and *rpoB'* gene (b) sequences and phylogenomic tree (c). Phylogenetic reconstruction was performed using MEGA 7.0, while phylogenomic tree was reconstructed using EasyCGTree. Neighbor-Joining (NJ), Maximum-Likelihood (ML) and Maximum-Parsimony (MP) algorithms were employed for the 16S rRNA gene and *rpoB'* gene phylogenetic analysis, while Maximum-Likelihood algorithm was employed for phylogenomic analysis. Percentage bootstrap values (> 50%) are shown at branch points. The accession numbers of the gene sequences or genomes are shown in the parentheses. "-" supporting rate below 50% or does not obtain this lineage. The numerical values separated by slashes (/) at the branch points represent the bootstrap supporting rate of the three distinct algorithms: ML, NJ, and MP, respectively. Bar represents expected substitutions per nucleotide position.

gene phylogenetic tree revealed subtle topological differences: *H. salinus* GX3^T preferentially clustered with *H. litoreus* GX26^T, forming a group that subsequently associated with PRR65^T to establish the characteristic lineage of the genus *Halorubellus* (Fig. 2b). The topology of the *Halorubellus* clade in the whole-genome phylogenomic tree showed remarkable similarity to that of the *rpoB'* gene tree (Fig. 2c) with a robust supporting rate (nearly 100%). Collectively, the phylogenetic position of PRR65^T within the genus *Halorubellus* remained relatively stable, indicating fundamental consistency in the genetic relationships revealed by 16S rRNA gene, *rpoB'* gene, and whole-genome sequence analyses.

Comparative genomics. The genomic comparison reveals numerous homologous regions among the genomes of the three strains (Fig. 3), along with some strain-specific DNA segments, which may be attributed to insufficient sequencing depth, incomplete genome sequences, or the adaptive evolution of the strains in different environments. The COG functional categories within strains PRR65^T, *H. salinus* GX3^T, and *H. litoreus* GX26^T showed that genes involved in Replication, recombination and repair, coenzyme transport and metabolism, defense mechanisms, cell cycle control, cell division, chromosome partitioning, Intracellular trafficking, secretion, and vesicular transport, were most abundant in strain PRR65^T. In contrast to other strains, strain PRR65^T possesses the smallest repertoire of genes involved in amino acid transport and metabolism, energy production and conversion, inorganic ion transport and metabolism, lipid transport and metabolism, nucleotide transport and metabolism, secondary metabolites biosynthesis, transport and catabolism, carbohydrate transport and metabolism, signal transduction mechanisms, cell wall/membrane/envelope biogenesis, and cell motility

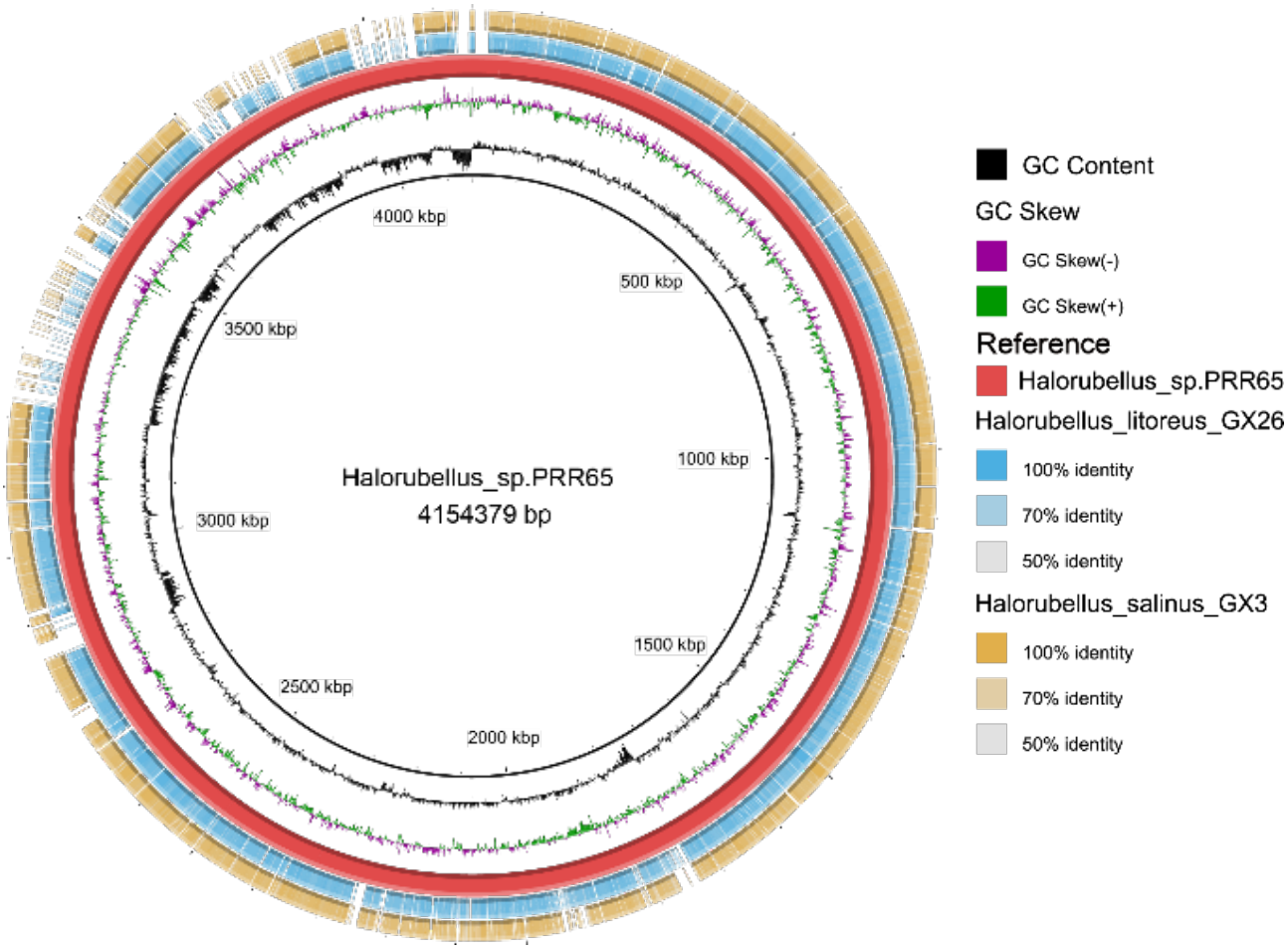

Fig. 3. Circular representation of the strain PRR65^T genome.
The Figure shows a draft strain PRR65^T genome compared against *Halorubellus litoreus* GX26^T and *Halorubellus salinus* GX3^T. The innermost rings show GC skew (purple/green) and GC content (black). The remaining rings show BLAST comparisons of the reference genome of strain PRR65^T (red), *H. litoreus* GX26^T (blue), and *H. salinus* GX3^T (yellow). The dashed line shows the region with relatively low DNA G + C content differentiated from other regions.

Table III
Average amino acid identity (AAI) between strain PRR65 and its closely related species.

Strain	AAI (%)
Halorubellus salinus GX3	86.32
Halorubellus litoreus GX26	86.47
Halomicrococcus hydrotolerans H22	79.43
Haloarchaeobius salinus YC82	79.21
Haloarchaebius iranensis KCTC 4080	77.56
Haloarchaebius amylolyticus XD48	76.13

(Fig. 4). The primary functional association of these genes lies in cellular metabolic processes. Genomic comparison of the three presently described species within the genus *Halorubellus* reveals 2,466 conserved core genes. Strain-specific gene counts are 325 for *H. litoreus* GX26^{T}, 225 for strain PRR65^{T}, and 142 for *H. salinus* GX3^{T}. The pan-genome constructed from these isolates contains 2,158 gene clusters.

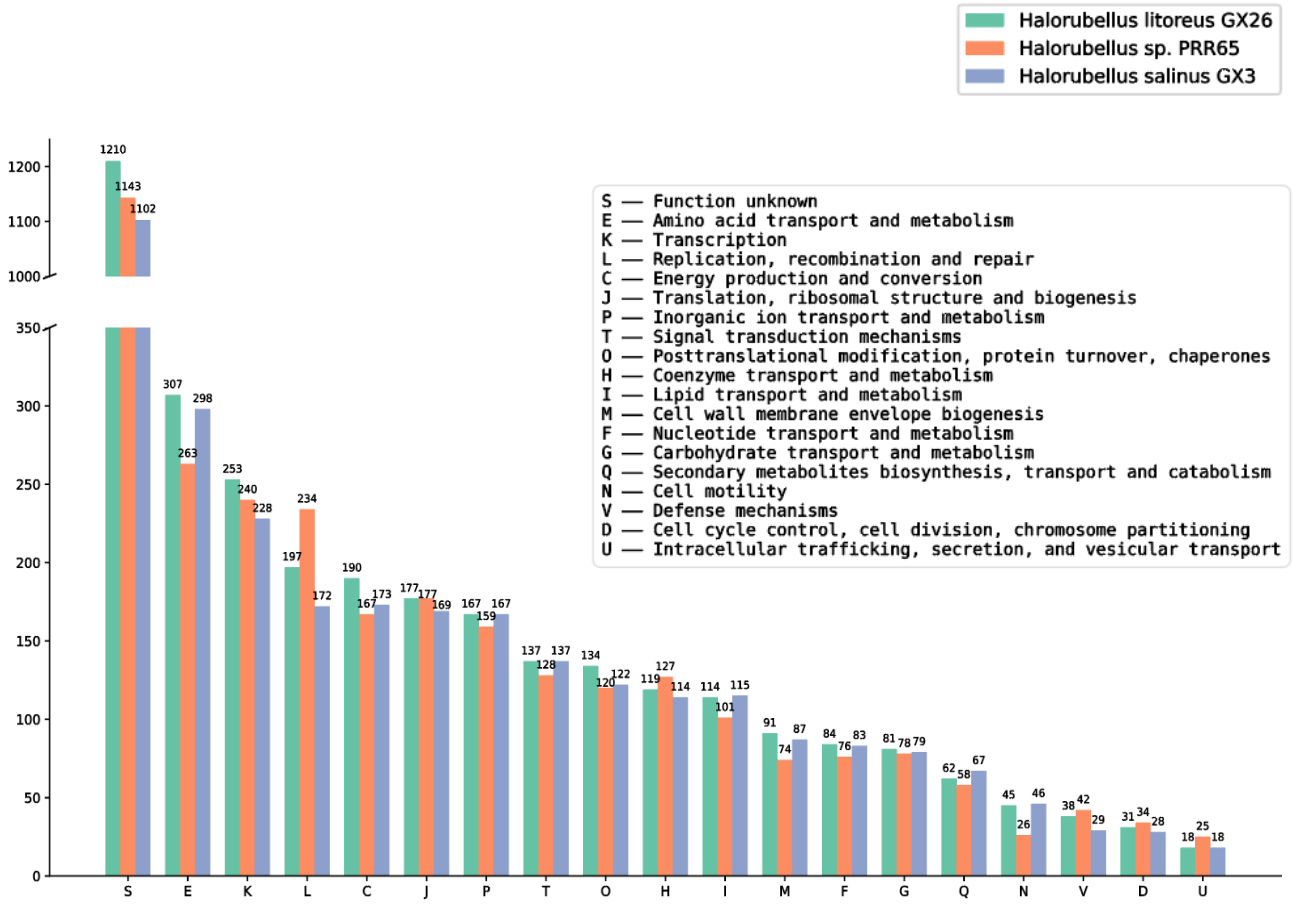

Fig. 4. The distribution of gene counts across COG functional categories in three *Halorubellus* strains, illustrated by a bar chart. The x-axis represents COG categories, and the y-axis indicates the number of genes assigned to each category based on genome annotation. Functional annotation was performed using the eggNOG-mapper v2 platform, with assignments based on the eggNOG database. Bar colors denote different strains: green for *Halorubellus litoreus* GX26^{T}, orange for strain PRR65^{T}, and blue for *Halorubellus salinus* GX3^{T}. Functional descriptions of each COG category are displayed in the top-right corner of the figure.

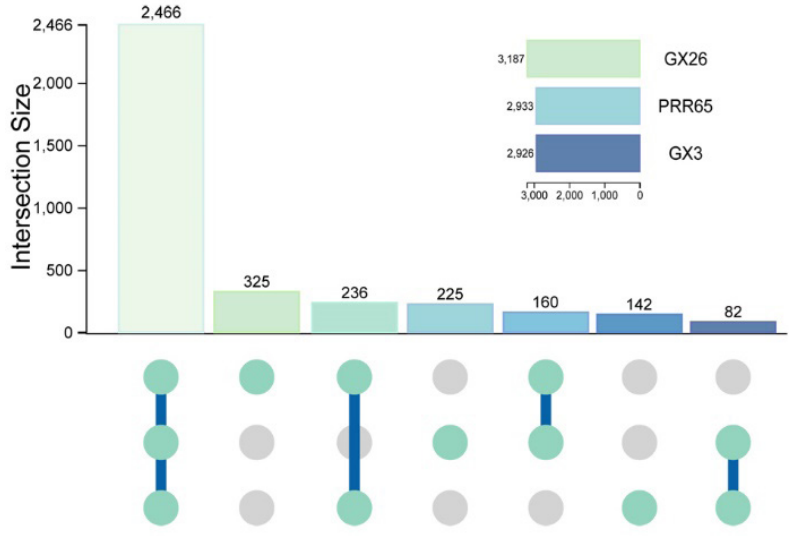

Fig. 5. Upset Venn diagram from the pan - genome analysis of strain PRR65^T, *Halorubellus litoreus* GX26^T, and *Halorubellus salinus* GX3^T. Gene statistical analysis was performed on the genomes of these three species. The diagram illustrates the distribution and intersection of genes among the species. The bar chart at the upper - right shows the gene number statistics for each species (species names: Strain PRR65^T, *H. litoreus* GX26^T, and *H. salinus* GX3^T are marked in the legend). Single points in the middle matrix represent unique elements specific to certain sets. The lines connecting the points represent the unique intersections of different sets. Vertical bar charts in different colors represent the corresponding intersection element values.

Conclusions

The phenotypic and chemotaxonomic properties, as well as sequence similarity and DNA-DNA relatedness, suggest that strain PRR65T represents a novel species in the genus *Halorubellus*, for which the name *Halorubellus amylolyticus* sp. nov. was proposed.

Description of *Halorubellus amylolyticus* sp. nov. *Halorubellus amylolyticus* (a.my.lo.ly′ ti.cus. Gr. neut. n. *amylon*, starch; Gr. masc. adj. *lytikos* dissolving; N.L. masc. adj. *amylolyticus*, starch-dissolving).

Halorubellus amylolyticus sp. nov. is a facultatively anaerobic archaeon capable of growth under oligotrophic conditions. It exhibits an obligately halophilic phenotype, requiring NaCl concentrations between 2.0–5.1 M for growth, with optimal proliferation observed at 3.4 M NaCl. The strain maintains viability across a pH spectrum of 5.5–9.0 (optimum pH 7.0) and a temperature range of 25–50°C (optimum 38°C). Cellular integrity is compromised in hypotonic environments, with complete lysis occurring in distilled water; a minimum of 1.7 M NaCl is required for membrane stabilization. Colonies on hypersaline media are pale red, moist, and opaque, reaching approximately 1.0 mm in diameter after standard incubation. Cells are Gram-stain-negative, motile, and exhibit a spherical morphology with diameters of 0.5–1.0 μm. The strain demonstrates catalase-positive but oxidase-negative activity. Under anaerobic conditions, growth is supported by nitrate as a terminal electron acceptor. DMSO cannot serve as a terminal acceptor, and anaerobic growth on L-arginine does not occur. The organism reduces nitrate to nitrite with concomitant gas production. Tests for indole formation and H_2S production yield negative results. Hydrolytic capabilities include degradation of casein, gelatin, and starch, while Tween 80 remains unhydrolyzed. The following compounds serve as sole carbon and energy sources: D-glucose, D-mannose, D-galactose, sucrose, starch, glycerol, mannitol, sorbitol, pyruvate, fumarate, glycine, L-alanine, L-arginine, L-aspartate, and L-glutamate. In contrast, no growth is supported by D-fructose, L-sorbose, D-ribose, D-xylose, maltose, lactose, acetate, lactate, succinate, malate, L-lysine, or L-ornithine. The polar lipid profile comprises phosphatidic acid (PA), phosphatidylglycerol (PG), phosphatidylglycerol phosphate methyl ester (PGP-Me), sulfated mannosyl glucosyl diether (S-DGD-1), mannosyl glucosyl diether (DGD-1), and sulfated galactosyl mannosyl glucosyl diether (S-TGD-1) as major components. The complete genome sequence reveals a DNA G + C content of 67.2 mol%. The type strain PRR65^T (= MCCC 4K00175 = KCTC 4323) was isolated from salt crystals adhering to commercially prepared salted seaweed knots (Wuhu, Anhui Province, China).

ORCID
Shaoxing Chen https://orcid.org/0000-0002-3695-9622

Availability of data and material
The accession numbers of *rpoB'* gene and genome for strain PRR65^{T} are PP981526.1 and GCA_034808145.1, respectively.

Acknowledgments
We would like to thank Dr. Daofeng Zhang from Hohai University and Prof. Wenjun Li from SUN YAT-SEN University for their help in construction the phylogenomic tree and constructive suggestions.

Author contributions
Yawen Liu, Aodi Zhang, Jinqiang Ma, Cunlong Lu, Shilong Shao, Yuling Hao, Yu Jin and Jingfang Liu performed the experiments. Aodi Zhang, Jinqiang Ma and Yue Ding analyzed the data. Liang Shen and Shaoxing Chen supervised this study. Shaoxing Chen wrote and revised the manuscript. All authors have read and approved the final manuscript.

Funding
This work was supported by grants from the Natural Science Foundation of Anhui Province, China (2208085MC39), the Outstanding Innovative Research Team for Molecular Enzymology and Detection in Anhui Provincial Universities (2022AH010012), the Yunnan Key Laboratory for Fungal Diversity and Green Development, Kunming Institute of Botany, Chinese Academy of Sciences, and the Second Tibetan Plateau Scientific Expedition and Research Program (STEP 2024QZKK0201).

Conflict of interest
The authors do not report any financial or personal connections with other persons or organizations, which might negatively affect the contents of this publication and/or claim authorship rights to this publication.

Literature

Aiyar A. The use of CLUSTAL W and CLUSTAL X for Multiple Sequence Alignment. Methods Mol Biol. 2000;132:221–241. https://doi.org/10.1385/1-59259-192-2:221

Baker BA, Gutiérrez-Preciado A, Rodríguez Del Río Á, McCarthy CGP, López-García P, Huerta-Cepas J, Susko E, Roger AJ, Eme L, Moreira D. Expanded phylogeny of extremely halophilic archaea shows multiple independent adaptations to hypersaline environments. Nat Microbiol. 2024;9(4):964–975. https://doi.org/10.1038/s41564-024-01647-4

Brown J, Pirrung M, McCue LA. FQC Dashboard: integrates FastQC results into a web-based, interactive, and extensible FASTQ quality control tool. Bioinformatics. 2017;33(19):3137–3139. https://doi.org/10.1093/bioinformatics/btx373

Chen S, Liu HC, Zhao D, Yang J, Zhou J, Xiang H. *Halorubrum yunnanense* sp. nov., isolated from a subterranean salt mine. Int J Syst Evol Microbiol. 2015;65(12):4526–4532. https://doi.org/10.1099/ijsem.0.000605

Cline SW, Schalkwyk LC, Doolittle WF. Transformation of the archaebacterium *Halobacterium volcanii* with genomic DNA. J Bacteriol. 1989;171(9):4987–4991. https://doi.org/10.1128/jb.171.9.4987-4991.1989

Cui HL, Gao X, Yang X, Xu XW. *Halorussus rarus* gen. nov., sp. nov., a new member of the family *Halobacteriaceae* isolated from a marine solar saltern. Extremophiles. 2010;14(6):493–499. https://doi.org/10.1007/s00792-010-0329-0

Cui HL, Hou J, Amoozegar MA, Dyall-Smith ML, de la Haba RR, Minegishi H, Montalvo-Rodriguez R, Oren A, Sanchez-Porro C, Ventosa A, et al. Proposed minimal standards for description of new taxa of the class Halobacteria. Int J Syst Evol Microbiol. 2024;74(3):006290. https://doi.org/10.1099/ijsem.0.006290

Cui HL, Mou YZ, Yang X, Zhou YG, Liu HC, Zhou PJ. *Halorubellus salinus* gen. nov., sp. nov. and *Halorubellus litoreus* sp. nov., novel halophilic archaea isolated from a marine solar saltern. Syst Appl Microbiol. 2012;35(1):30–34. https://doi.org/10.1016/j.syapm.2011.08.001

Ding Y, Ke J, Hong T, Zhang A, Wu X, Jiang X, Shao S, Gong M, Zhao S, Shen L, et al. Microbial diversity and ecological roles of halophilic microorganisms in Dingbian (Shaanxi, China) saline-alkali soils and salt lakes. BMC Microbiol. 2025;25(1):287. https://doi.org/10.1186/s12866-025-03997-3

Dussault HP. An improved technique for staining red halophilic bacteria. J Bacteriol. 1955;70(4):484–485. https://doi.org/10.1128/jb.70.4.484-485.1955

Goris J, Konstantinidis KT, Klappenbach JA, Coenye T, Vandamme P, Tiedje JM. DNA-DNA hybridization values and their relationship to whole-genome sequence similarities. Int J Syst Evol Microbiol. 2007;57(Pt_1):81–91. https://doi.org/10.1099/ijs.0.64483-0

Hall TA. BioEdit: A user-friendly biological sequence alignment editor and analysis program for Windows 95/98/NT. Nucleic Acids Symp Ser. 1999;41:95–98.

Hao Y, Jin Y, Zhang A, Jiang X, Gong M, Lu C, Pan R, Chen S. Identification and biochemical characterization of a novel halolysin from *Halorubellus* sp. PRR65 with a relatively high temperature activity. World J Microbiol Biotechnol. 2024;40(11):340. https://doi.org/10.1007/s11274-024-04149-x

Kim M, Oh HS, Park SC, Chun J. Towards a taxonomic coherence between average nucleotide identity and 16S rRNA gene sequence similarity for species demarcation of prokaryotes. Int J Syst Evol Microbiol. 2014;64(Pt_2):346–351. https://doi.org/10.1099/ijs.0.059774-0

Kumar S, Stecher G, Tamura K. MEGA7: Molecular Evolutionary Genetics Analysis version 7.0 for bigger datasets. Mol Biol Evol. 2016;33(7):1870–1874. https://doi.org/10.1093/molbev/msw054

Minegishi H, Kamekura M, Itoh T, Echigo A, Usami R, Hashimoto T. Further refinement of the phylogeny of the *Halobacteriaceae* based on the full-length RNA polymerase subunit B' (*rpoB'*) gene. Int J Syst Evol Microbiol. 2010;60(Pt_10):2398–2408. https://doi.org/10.1099/ijs.0.017160-0

Parks DH, Imelfort M, Skennerton CT, Hugenholtz P, Tyson GW. CheckM: assessing the quality of microbial genomes recovered from isolates, single cells, and metagenomes. Genome Res. 2015;25(7):1043–1055. https://doi.org/10.1101/gr.186072.114

Prjibelski A, Antipov D, Meleshko D, Lapidus A, Korobeynikov A. Using SPAdes de novo assembler. Curr Protoc Bioinformatics. 2020;70(1):e102. https://doi.org/10.1002/cpbi.102

Richter M, Rosselló-Móra R. Shifting the genomic gold standard for the prokaryotic species definition. Proc Natl Acad Sci U S A. 2009;106(45):19126–19131. https://doi.org/10.1073/pnas.0906412106

Seemann T. Prokka: Rapid prokaryotic genome annotation. Bioinformatics. 2014;30(14):2068–2069. https://doi.org/10.1093/bioinformatics/btu153

Ventosa A, de la Haba RR, Sánchez-Porro C, Papke RT. Microbial diversity of hypersaline environments: A metagenomic approach. Curr Opin Microbiol. 2015;25:80–87. https://doi.org/10.1016/j.mib.2015.05.002

Zhang DF, He W, Shao Z, Ahmed I, Zhang Y, Li WJ, Zhao Z. EasyCGTree: A pipeline for prokaryotic phylogenomic analysis based on core gene sets. BMC Bioinformatics. 2023;24(1):390. https://doi.org/10.1186/s12859-023-05527-2

Zhou Z, Charlesworth J, Achtman M. Accurate reconstruction of bacterial pan- and core genomes with PEPPAN. Genome Res. 2020;30(11):1667–1679. https://doi.org/10.1101/gr.260828.120

Supplementary materials are available on the journal's website.